actuators

MDPI

Article

Dielectric Elastomer Actuators with Carbon Nanotube Electrodes Painted with a Soft Brush

Hiroki Shigemune [1,*], Shigeki Sugano [2], Jun Nishitani [3], Masayuki Yamauchi [3], Naoki Hosoya [3], Shuji Hashimoto [1] and Shingo Maeda [3,*]

1 School of Advanced Science and Engineering, Department of Applied Physics, Waseda University, Tokyo 169-8050, Japan; shuji@waseda.jp
2 School of Creative Science and Engineering, Department of Modern Mechanical Engineering, Waseda University, Tokyo 169-8050, Japan; sugano@waseda.jp
3 Department of Engineering Science and Mechanics, Shibaura Institute of Technology, Tokyo 135-8548, Japan; ab13068@shibaura-it.ac.jp (J.N.); ab11108@shibaura-it.ac.jp (M.Y.); hosoya@sic.shibaura-it.ac.jp (N.H.)
* Correspondence: hshige@sawada.phys.waseda.ac.jp (H.S.); maeshin@shibaura-it.ac.jp (S.M.); Tel.: +81-(3)-5286-3233 (H.S.)

Received: 5 July 2018; Accepted: 21 August 2018; Published: 22 August 2018

Abstract: We propose a simple methodology to paint carbon nanotube (CNT) powder with a soft brush onto an elastomer. A large deformation of dielectric elastomer actuator (DEA) occurs according to the small constraint of the electrodes. Uniform painting with a soft brush leads to a stable deformation, as demonstrated by the results of multiple trials. Unexpectedly, painting with a soft brush results in aligned materials on the elastomer. The oriented materials demonstrate anisotropic mechanical and electronic properties. This simple methodology should help realize innovative DEA applications.

Keywords: additive manufacturing; dielectric elastomer actuator; brush painting

1. Introduction

Soft actuators and their applications have been studied in a variety of perspectives. Examples include pneumatic soft rubber actuators [1–4], dielectric elastomer actuators (DEAs) [5–8], and gel actuators [9,10]. Compared to other soft actuators, DEAs are energy efficient and power dense because they are electrostatic actuators. Additionally, DEAs are lightweight and operate silently. For these reasons, DEAs are attracting attention in both research and industrial fields. Companies are beginning to employ DEA technologies to adopt the energy efficiency. Valves and grippers of DEAs are demonstrated [11].

Figure 1 shows the structure of DEA as a capacitor due to the electrostatic driving mechanism. Applying a voltage difference across the stretchable electrodes causes a squeeze as the stretchable electrodes pull against each other. This squeeze contracts the actuator in the thickness direction and expands it in the plane direction due to the incompressibility of the rubber. Simply stacking and actuating the rubber and the electrodes can realize a few percent of actuated strain.

One potential application with a small deformation is a speaker. Hosoya et al. demonstrated hemispherical breathing mode speakers using non–pre-strained DEA composed of silicone rubber [12]. Pre-straining can enhance the actuated strain. In 2000, Pelrine et al. reported that the actuation strains in pre-strained DEAs exceed 100%, demonstrating that the displacement of pre-strained DEAs is much larger than that of non-pre-strained ones [5]. Additionally, research related to pre-strained DEAs, such as theoretical models and materials and device integrations, are recognized as a prospective designing method for practical applications.

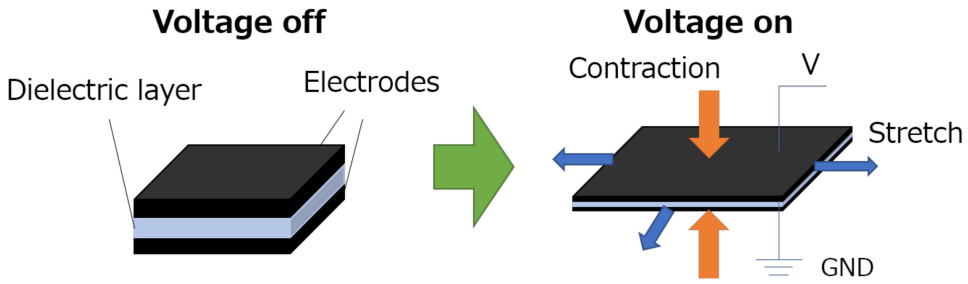

Figure 1. Driving principle of the dielectric elastomer actuator (DEA). DEA employs stretchable rubber as the dielectric of the capacitor and stretchable electrodes. Applying a voltage difference to the stretchable electrodes squeezes the stretchable rubber. Rubber contracts in the thickness direction and expands in the plane direction due to incompressibility of the rubber.

The main issue of DEAs is a high driving voltage. The high voltage restricts applications due to requirement of voltage amplifier and safety reasons. Two approaches have been considered to overcome these issues. One is to configure a thinner dielectric layer and the other is to reduce strain constraint of the electrode layer. Considering a DEA simple model, the characteristic strain of actuation s is given by [13]

$$s = -\frac{\epsilon_r \epsilon_0 V^2}{Y d^2} \tag{1}$$

where ϵ_r and ϵ_0 are permittivity of the relative and vacuum; Y, V, and d are the Young's modulus, an applied voltage, and a thickness of the dielectric rubber, respectively. Equation (1) determines the displacement of DEAs. From Equation (1), reducing the thickness of the dielectric rubber lowers the driving voltage of DEAs.

Interestingly, Shea's group recently reported a strain of 7.5% with a driving voltage of 245 V using a 3-µm-thick dielectric layer [8]. However, there exists limitations in fabrication process to create a thinner dielectric layer. For example, a thinner layer is torn easily and is difficult to remove when the film is stuck. In this study, we aim to improve performance of the DEA by reducing the strain constraints of the electrode layer.

It is well known that the performance of DEA strongly depends on the conditions of the stretchable electrodes. Unless the electrodes stretch better than the rubber in the dielectric layer, the actuation is constrained by the electrodes. There are four types of materials for DEA electrodes (ionic gels [14], carbon grease [15], conductive rubbers [8], and carbon powders [16]). Compared to the other types of electrodes, stretchable electrodes made of ionic gels are highly transparent [14]. However, they suffer from leakage of water and bonding issues between the rubber and the gel.

Carbon grease is easy to handle, but maintaining its shape is quite difficult due to the fact that it is a viscous liquid [15]. Carbon grease is easy to dry and easy to spread on a dielectric rubber, and the oil components affect a dielectric rubber gradually. Researchers have reported using conductive rubbers as stretchable electrodes [8]. The researchers emerge a conductive carbon powder by mixing a carbon black and a flexible polymer to obtain flexible electrodes, which are quite stable for DEAs. The advantage of this method is that DEAs can be fabricated via printing. Shea's group has established systematic printing methods for DEAs using conductive rubber, which is noteworthy [17]. However, Equation (1) does not describe an actuation property in the case of DEA with conductive rubber electrodes. The equation should include terms to express that the material properties of conductive rubber, such as thickness and hardness [18], restricting the actuation.

On the other hand, electrodes made with the carbon powders are ideal to research DEAs with large actuations because the effect of thickness and hardness of the electrodes to the actuation is small compared to the other electrodes. However, coating, patterning, and printing methods of powders are not well investigated. Several carbon powders such as carbon black, carbon nanotubes (CNTs), and graphite are used for electrodes of DEAs. Herein, we focus on CNTs because they have

interesting properties compared to other carbons. CNTs change the material properties up to a number of layers (multi-walled, single-walled) and curling patterns (metal and semiconductor). Fabrication and separation processes for CNTs have been developed as an alternative to existing silicone-based materials. Furthermore, CNTs display a large anisotropic property, which other carbon-based powders lack. The longitudinal length of CNT is ~1000 times longer than the shorter direction in our case (multi-walled carbon nanotube 724769, Sigma-Aldrich, Saint Louis, MO, USA). Aligned CNTs show an anisotropic electrical property. The conductivity changes about 60 times according to the direction of the patterned CNTs [19]. When the substrate is stretched in the longitudinal direction, the conductivity can effectively persist in the tube configuration. The CNTs slide by stretching and it is unlikely that contact between CNTs is completely lost.

Several methods have been proposed to print CNTs by mixing into a solution, including painting [20], spraying [21], and inkjet printing [22]. Inkjet printing is a promising method to draw complex pattern conveniently, especially when a desktop inkjet printer is employed. A desktop inkjet printer has an arguable affinity with a prototype mechatronic system [23]. Three-dimensional (3D) wiring board printed with an inkjet printer was also proposed [24]. Generally, CNTs are dispersed into solutions to apply these printing methods. However, CNTs easily aggregate due to their strong van der Waals force, making it difficult to create high-density CNT ink. Some researchers have added functional groups to CNTs to try to make them soluble. However, chemical modifications can deteriorate the properties of CNTs. Wettability between the substrate and the solution is also not negligible. Non-uniform patterning due to the coffee ring effect, which is caused by differential evaporation of the droplet, should be managed.

Direct patterning of the CNT powder can be an alternative method to bypass the aforementioned issues. In this study, we propose a simple concept of painting a CNT powder directly on an elastomer with a soft brush. Painting tools are used not only in industrial fields but also in daily life, to pattern various inks, and are deeply related to human culture, such as arts and calligraphy [25].

2. Materials and Methods

Figure 2a shows a soft brush employed in experiments. The soft brush consists of aligned high-density hairs with a 150-μm diameter and a Young modulus of 10.53 GPa. The hairs buckle when painting on the staffs, providing a uniform force onto the substrate. Changing the painting direction can control the force vector. This simple method enhances and manages the driving property, expanding the potential of DEA applications. There were two types of elastomers: acrylic and silicone. Generally, DEAs with acrylic elastomers show a high deformation and a slow transient, whereas DEAs with silicone elastomers show a small deformation and a fast-transient speed. Which elastomer to choose depends on the applications. Figure 2b shows schematic of the DEA pattern electrode process. Teflon sheet was employed as a masking sheet to design circular CNT electrodes.

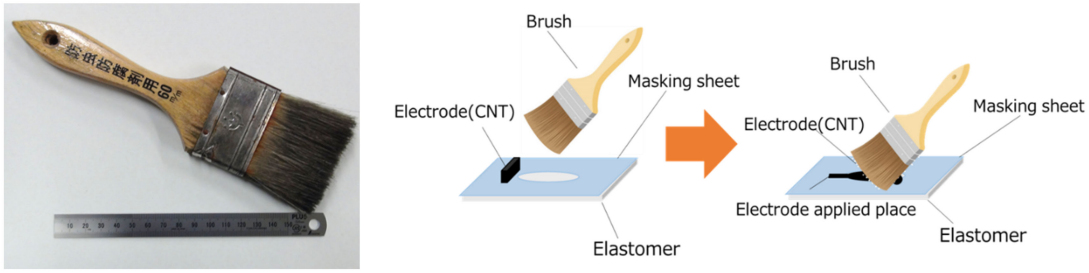

(**a**) (**b**)

Figure 2. (**a**) Photo of a soft brush employed to paint DEA electrodes. It consists of aligned high-density hairs with a 150-μm diameter and a 10.53 GPa Young modulus. (**b**) Schematic of process to pattern the electrodes. Sheet of Teflon is used to pattern the electrodes.

We summarize materials and methods employed for experiments in Table 1. We employed an acrylic elastomer (VHB Y-4905J, 3M, Maplewood, MN, USA) and a silicone elastomer (ELASTOSIL FILM 2030 SHEET, WACKER, Munich, German). The acrylic elastomer has a feature in configuration. The elastomer is used as an adhesive tape, and sandwiched by adhesive layers. The existence of the adhesive layers highly affects to results. We applied CNT (multi-walled carbon nanotube 724769, Sigma-Aldrich, Saint Louis, MO, USA) to the elastomers by hand and the brush. For painting by hand, we employed tissue paper to transfer the CNT powder. We put certain amount of the powder to the tissue paper, and apply the powder to the elastomer by hand. The tools used for the painting is shown in the last line of Table 1.

Table 1. Materials and methods employed in the experiment.

	DEA A	**DEA B**	**DEA C**
Material of elastomer	Acrylic	Acrylic	Silicone
Model number (Supplier)	VHB Y-4905J (3M)	VHB Y-4905J (3M)	ELASTOSIL FILM 2030 SHEET (WACKER)
Painting tool	Hand	Brush	Brush

2.1. Observation Experiment

Firstly, we conducted observation experiments to investigate the conditions of the electrode on the elastomers. We brushed CNT powders in one direction onto surface of the elastomers which are pre-stretched. We pre-stretched all the acrylic DEAs demonstrated in the paper for 300% using an aluminum frame on all sides. The silicone DEA was pre-stretched 50% using the same method.

We took images with a camera and a Scanning Electron Microscopy (SEM) (VE9800, Keyence, Osaka, Japan). For the images taken with the camera, we analyzed with a gray scale histogram of the image. Pixels corresponded to each color of the gray scale were counted by an image analysis software (Image J). We employed a white background to observe transparency of the electrode. We evaluated the electrode from two factors, which were intensity of peak in the histogram and value of gray scale which has the largest value. Uniformity of the electrode was investigated from the intensity of peak in the histogram. Transparency was examined from the value of gray scale which has the largest value. For the images taken with the SEM, we analyzed distribution of the orientation using image analysis software based on fast Fourier transfer [26]. As a control experiment, we applied the brush to the acrylic elastomer without CNT. Then, we stroked the brush on the acrylic elastomer for 120 times to confirm whether existence of the CNT was required for the orientation.

2.2. Performance Experiment

Secondly, we investigated the performance of DEAs. We conducted three experiments to compare performance of the DEA of which electrodes painted by hand and the brush. (1) We measured transient response of the DEAs. We applied a voltage of 2 kV for 3000 s to the DEAs listed in Table 1. (2) We compared static strain of the DEAs. A voltage between 0.5 kV and 2 kV was applied to the acrylic elastomer of which the electrodes were painted by hand or with the brush. We measured the radial strain 3000 s after applying the voltage. (3) Stability of the actuation was also investigated. We attempted the experiment to measure the static strain five times with applied a voltage of 2 kV, and took average and error of the attempts to examine the reproductivity. The radial strains were measured by the image analysis software (Image J) in the three experiments. We employed an amplifier (HEOPT-20B10, Matsusada Precision Inc., Shiga, Japan) to apply high voltage for the actuator.

Finally, we conducted experiments to observe the effect of oriented CNTs on the mechanical and electrical properties of DEA. As mentioned in the introduction, anisotropy is one of notable features of CNTs. Anisotropy can be induced by painting with the brush in one direction. A 300% pre-stretched

acrylic elastomer was coated by CNT with brushing in one direction. A square electrode with 7 cm sides was employed to observe the anisotropic property. We applied voltage of 2 kV to the DEA for 3000 s. The center of each side was captured with the image analysis software to obtain lateral strain. We also measured the anisotropic resistance of electrodes. A 5-cm square electrode was prepared, and the resistances were measured parallel and perpendicular to direction of the orientation direction.

3. Results and Discussions

3.1. Observation Experiment

We patterned the circular electrodes by hand (Figure 3a) and painted with the soft brush (Figure 3b) through the masking sheet. Figure 4a,b show the histogram results from the electrode patterned by hand and the brush. Values of vertical axis are standardized by the maximum value in the graph. The histogram from the brushed electrodes shows larger value of gray scale and a higher intensity peak than from the electrode patterned by hand. The painting sequence removes the extra CNTs on the electrodes. Consequently, the electrode has a uniform density and a high transparency.

Figure 5a shows photo of the electrode on the silicone elastomer. We painted CNT powders on the silicone elastomer to investigate the substrate dependence. A gray histogram in Figure 5b shows that uniform patterning is also achieved for the silicone elastomer. The electrode on the silicone elastomer is more transparent compared to the one on an acrylic elastomer. This is because the adhesive layer stacks on the acrylic elastomer, but not on the silicone elastomer. CNTs attach to the adhesive layer, and eventually more CNTs remain on the acrylic elastomer. Table 2 shows feature values of the gray scale histograms. The electrode painted by the brush showed higher mean value and smaller standard deviation than the electrode painted by hand. Thus, the electrode painted by the brush was more uniform and transparent.

Figure 6 shows SEM photos of CNT powders painted on the acrylic elastomer by hand (Figure 6a), on the acrylic elastomer with the soft brush (Figure 6b), and on the silicone elastomer painted with the soft brush (Figure 6c). We observed orientation of material on the acrylic elastomers in one direction. The direction was equivalent to the applied brush direction. On the other hand, we were unable to observe the orientation on the silicone elastomer. Figure 6d–f show distribution of the orientations. The specimen with the acrylic elastomer shows a high intensity in one angle.

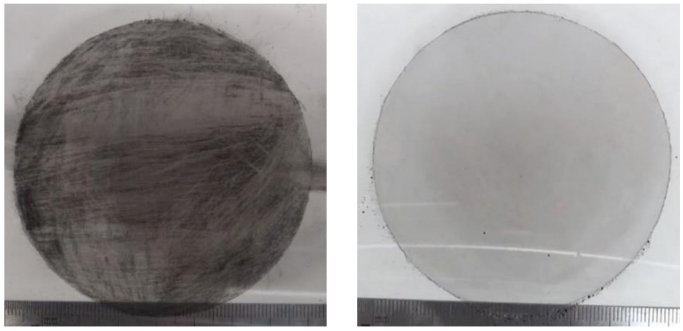

(**a**) (**b**)

Figure 3. (**a**) A stretchable electrode patterned by hand on the acrylic elastomer. (**b**) A stretchable electrode painted with the soft brush on the acrylic elastomer. A uniform and transparent electrode was obtained by painting with the soft blush.

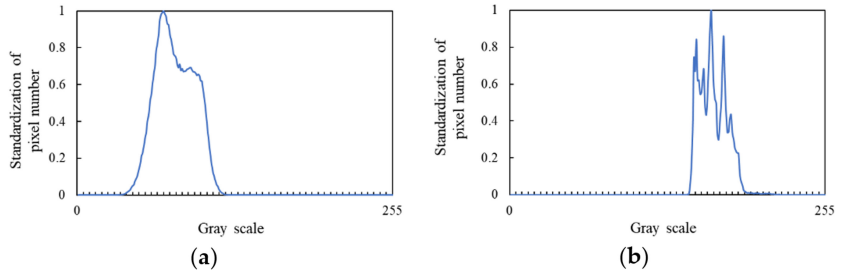

Figure 4. Gray scale histogram of (**a**) a stretchable electrode patterned by hand on the acrylic elastomer and (**b**) a stretchable electrode painted with the soft brush on the acrylic elastomer. The histogram from the brushed electrodes shows a larger value of gray scale and a higher intensity peak.

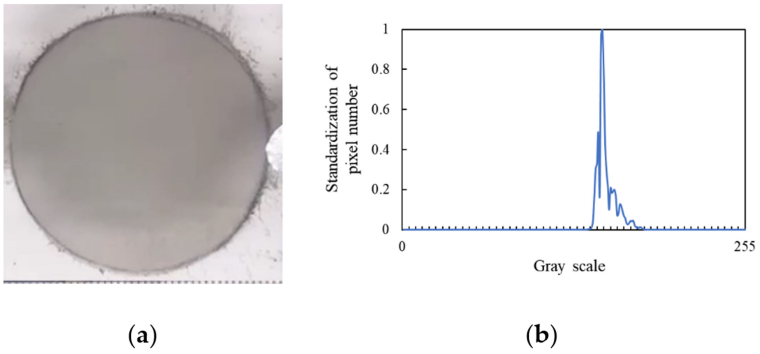

Figure 5. (**a**) A stretchable electrode painted with the soft brush on a silicone elastomer. (**b**) Gray scale histogram of the photo. The graph shows more intense peak compared to the electrode placed on the acrylic elastomer.

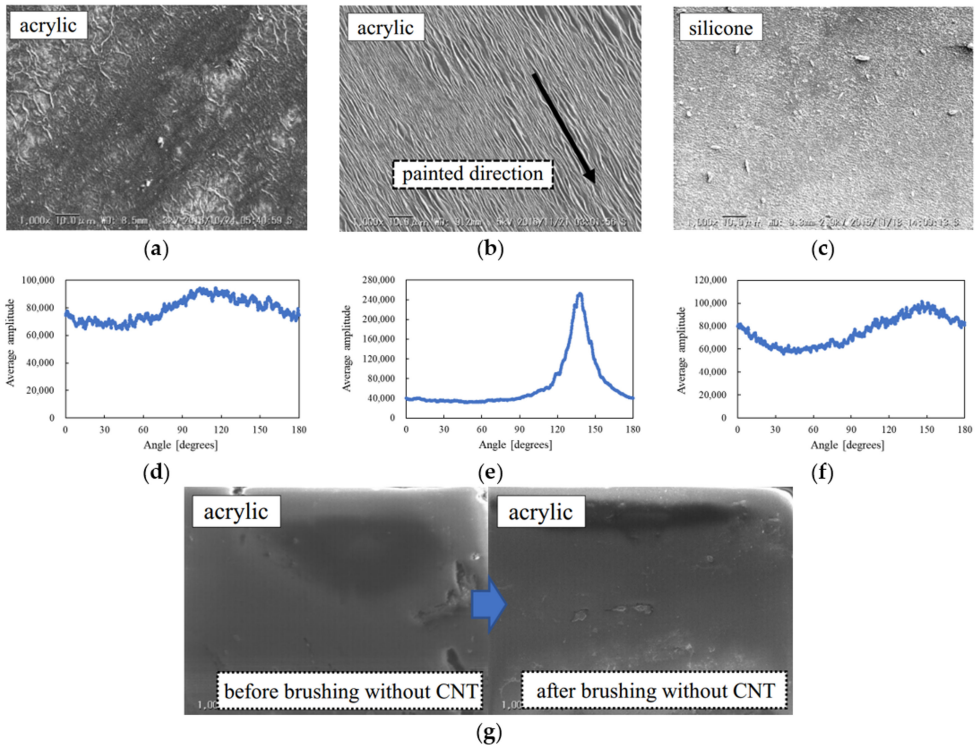

Figure 6. SEM images and graphs of orientation distributions on the acrylic elastomer (**a**,**d**) painted by hand; (**b**,**e**) painted with the soft blush; and (**c**,**f**) the silicone elastomer painted with the soft blush.

Orientation of a material is observed on a surface of the acrylic elastomer painted with the soft blush. (**g**) SEM images of the acrylic elastomer surface before and after painting 120 times with the soft brush without carbon nanotube (CNT) powder.

Table 2. Feature values of histograms.

	DEA A	DEA B	DEA C
Max value	122	217	179
Minimum value	33	56	137
Mean value	78.5	164	151
Standard deviation	15.3	11.1	6.65

We hypothesized that the orientation was induced by flowing or scarring of the adhesive layer. Figure 6g shows images when the soft brush is applied directly on the acrylic elastomer for 120 times without the CNT powder. We could not observe the deference between before and after applying the brush directly to the acrylic elastomer without CNT. From this result, we conclude that the orientation of the material observed in the SEM image relates to interaction between the elastomer and CNT. We supposed that the orientation of material affects performance of the DEA. The mechanical and electrical effects are investigated in the next subsection.

3.2. Performance Experiment

Figure 7 shows static driving states of an acrylic DEA painted with the soft brush. Figure 7a,b show reference and driving states respectively. The CNT electrodes stretch circularly as shown in the figures. Figure 8 shows dynamic response of the DEAs. The acrylic elastomer painted with the brush shows the largest radial strain (52%), which can be the rephrased area strain of 133% with applied a voltage of 2 kV. Painting the electrode with the brush provides a 13.7% larger strain than painting by hand in case of the acrylic elastomer. The silicone elastomer shows a fast-transient response compared to the acrylic elastomer. Radial strain of 5.5% is obtained on the silicone elastomer painted with the brush.

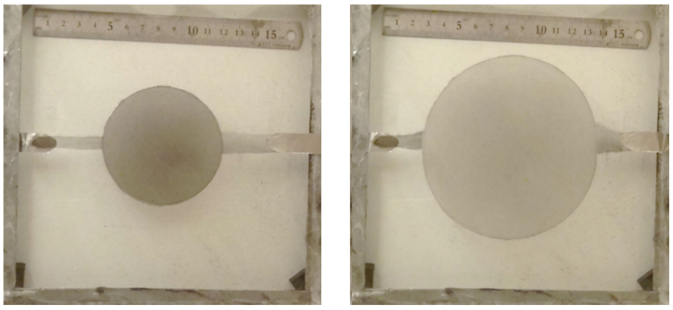

(**a**) (**b**)

Figure 7. (**a**) Reference (**b**) and driving state of the acrylic DEA painted with the soft brush. Terminal displacement of an acrylic DEA is visualized via 2-kV voltage applied for 3000 s. Acrylic DEA shows a radial strain of 52%, indicating a 133% area strain.

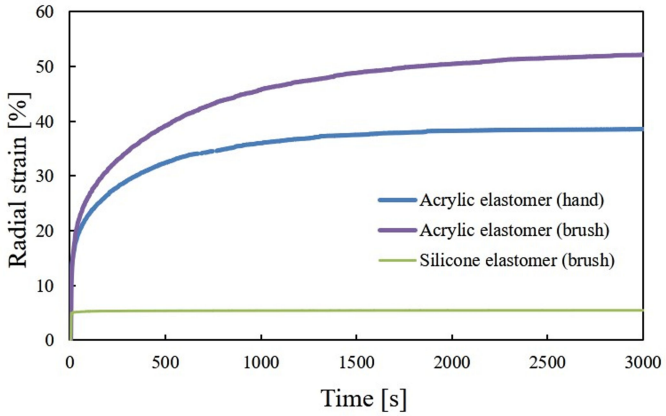

Figure 8. Dynamic response of the DEAs. The acrylic elastomer painted with the brush shows a 13.7% larger radial strain compared to an acrylic elastomer painted by hand. The silicone elastomer shows a fast transient response, which is a feature of the silicone elastomer itself.

Figure 9 shows trends in radial strains as a function of an applied voltage. The powder electrodes hardly restrict deformation of the elastomer, resulting in a larger deformation of the actuator. The larger deformation leads to deformation with a low voltage. To develop a DEA driven with the low voltage, selecting the property of the electrodes can be an alternative to fabricate thinner dielectric elastomers. For any applied voltages from 0.5 kV to 2 kV, the DEA painted with the brush exhibits better performance than that painted by hand. Applying a larger voltage (e.g., 2.5 kV) causes the DEAs to be broken down, and prevents to measure the static strain.

One of the advantages of the painting methods is reproducibility. We hypothesize that painting with the brush leads to stable actuation of the DEAs since uniform patterning of the electrodes realizes a uniform strain. Figure 10 shows the average radial strain of the DEAs over five trials. The error bars show the maximum and the minimum values. Differences of 11% and 6% in the error are obtained from the DEAs painted by hand and with the brush, respectively. Thus, painting DEAs with the soft brush results in larger displacement and higher reproducibility.

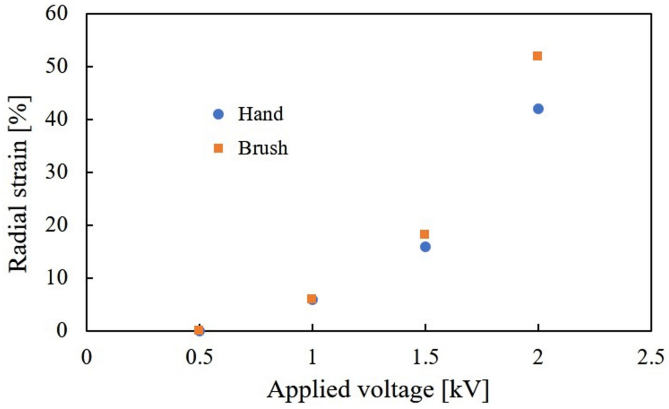

Figure 9. Radial strain of DEAs as a function of an applied voltage. For applied voltages between 0.5 kV and 2 kV, DEA painted with the brush shows larger strain.

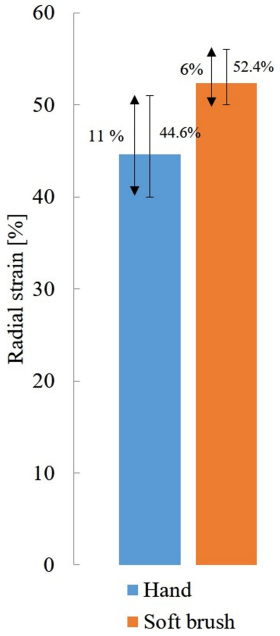

Figure 10. Average radial strains of the DEAs painted by hand and with the brush. Error bars show the maximum and the minimum values over five trials. The DEA painted with the soft brush shows larger strain and smaller error.

Figure 11 shows time transient of lateral strains perpendicular and parallel to the oriented direction of CNT. The DEA with the square electrode demonstrates anisotropic deformation. The deformation of the DEA perpendicular to the direction of the orientation shows larger strain than that in the parallel direction by 5.9% at 3000 s after applying the voltage. The deformation of the longer direction is restrained due to the high van der Waals force of CNTs. The resistances measured perpendicular and parallel to the orientation were confirmed as 2.58 MΩ and 5.56 MΩ, respectively. The resistance measured perpendicularly showed less value than the one with parallel by 46%. After applying a voltage of 1 kV to induce deformation, the resistances changed to 5.87 MΩ (perpendicular) and 4.72 MΩ (parallel), respectively. The change of the resistance would be caused by stretching of the elastomer due to the actuation and electric field generated by applying the voltage.

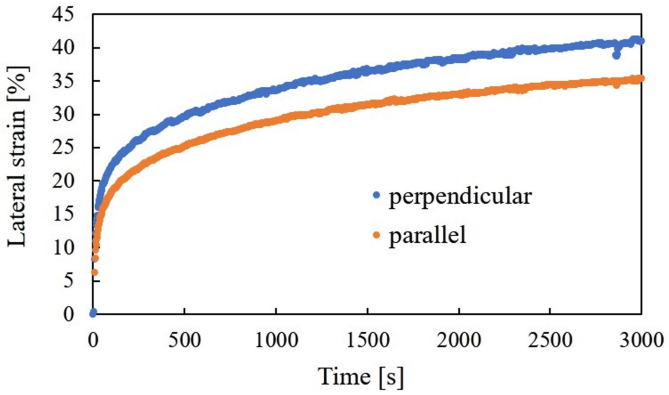

Figure 11. Time transient of lateral strains perpendicular and parallel to the orientation. A voltage of 2 kV was applied for 3000 s. The DEA demonstrates larger actuation in the perpendicular direction to the orientation.

4. Conclusions

In summary, we propose the simple methodology to paint CNT powder with the soft brush onto the elastomer. A large deformation of DEA for the radial strain of 52% occurs according to small constraint of the electrodes. Uniform painting with the soft brush leads to stable deformation, as demonstrated by the experiments with five trials. Unexpectedly, painting with the soft brush results in aligned material on the acrylic elastomer. The orientation occurs due to the adhesive layer sandwiching the layer of the acrylic elastomer. The adhesive nature interacts with materials to aggregate in one direction. The oriented CNTs show anisotropic mechanical and electronic properties. The lateral strain enlarges by 5.9% and the resistance decreased by 46% due to the orientation. Comparing with painting by hand, painting by the brush increases safeness of a human. A risk to interact the hazardous material decreases by using the brush. This simple methodology should help realize innovative DEA applications.

Author Contributions: Conceptualization: H.S., S.H., and S.M.; Data curation: J.N. and M.Y.; Investigation: H.S., N.H., and S.M.; Methodology: M.Y., N.H., and S.M.; Supervision: S.S., S.H., and S.M.; Writing-original draft, H.S. and S.M.

Funding: This research was supported in part by JSPS KAKENHI under Grant JP16J07902, JP16K14202, 16H04291, and 17K18858. This work is funded by Research Institute for Science and Engineering, Waseda University, and Shibaura Institute of Technology.

Conflicts of Interest: The authors declare no conflict of interest.

References

1. Suzumori, K.; Iikura, S.; Tanaka, H. Applying a flexible microactuator to robotic mechanisms. *IEEE Cont. Syst.* **1992**, *12*, 21–27.
2. Laschi, C.; Cianchetti, M.; Mazzolai, B.; Margheri, L.; Follador, M.; Dario, P. Soft robot arm inspired by the octopus. *Adv. Robot.* **2012**, *26*, 709–727. [CrossRef]
3. Cacucciolo, V.; Renda, F.; Poccia, E.; Laschi, C.; Cianchetti, M. Modelling the nonlinear response of fibre-reinforced bending fluidic actuators. *Smart Mater. Struct.* **2016**, *25*, 105020. [CrossRef]
4. Tolley, M.T.; Shepherd, R.F.; Mosadegh, B.; Galloway, K.C.; Wehner, M.; Karpelson, M.; Wood, R.J.; Whitesides, G.M. A resilient, untethered soft robot. *Soft Robot.* **2014**, *1*, 213–223. [CrossRef]
5. Pelrine, R.; Kornbluh, R.; Pei, Q.; Joseph, J. High-speed electrically actuated elastomers with strain greater than 100%. *Science* **2000**, *287*, 836–839. [CrossRef] [PubMed]
6. Carpi, F.; De Rossi, D.; Kornbluh, R.; Pelrine, R.E.; Sommer-Larsen, P. *Dielectric Elastomers As Electromechanical Transducers: Fundamentals, Materials, Devices, Models and Applications of an Emerging Electroactive Polymer Technology*; Elsevier: Amsterdam, The Netherlands, 2008; ISBN 978-0-08-047488-5.
7. Suo, Z. Theory of dielectric elastomers. *Acta Mech. Solida Sin.* **2010**, *23*, 549–578. [CrossRef]
8. Poulin, A.; Rosset, S.; Shea, H.R. Printing low-voltage dielectric elastomer actuators. *Appl. Phys. Lett.* **2015**, *107*, 244104. [CrossRef]
9. Maeda, S.; Hara, Y.; Sakai, T.; Yoshida, R.; Hashimoto, S. Self-walking gel. *Adv. Mater.* **2007**, *19*, 3480–3484. [CrossRef]
10. Nakagawa, H.; Hara, Y.; Maeda, S.; Hashimoto, S. A pendulum-like motion of nanofiber gel actuator synchronized with external periodic pH oscillation. *Polymers* **2011**, *3*, 405–412. [CrossRef]
11. DIELASTAR Research Project. Available online: https://www.festo.com/group/en/cms/10274.htm (accessed on 3 August 2018).
12. Hosoya, N.; Baba, S.; Maeda, S. Hemispherical breathing mode speaker using a dielectric elastomer actuator. *J. Acoust. Soc. Am.* **2015**, *138*, 424–428. [CrossRef] [PubMed]
13. Pelrine, R.; Kornbluh, R.; Joseph, J. Electrostriction of polymer dielectrics with compliant electrodes as a means of actuation. *Sens. Actuators A Phys.* **1998**, *64*, 77–85. [CrossRef]
14. Keplinger, C.; Sun, J.Y.; Foo, C.C.; Rothemund, P.; Whitesides, G.M.; Suo, Z. Stretchable, transparent, ionic conductors. *Science* **2013**, *341*, 984–987. [CrossRef] [PubMed]
15. Pelrine, R.; Kornbluh, R.; Joseph, J.; Heydt, R.; Pei, Q.; Chiba, S. High-field deformation of elastomeric dielectrics for actuators. *Mater. Sci. Eng. C.* **2000**, *11*, 89–100. [CrossRef]

16. Lochmatter, P.; Kovacs, G. Design and characterization of an active hinge segment based on soft dielectric EAPs. *Sens. Actuators A Phys.* **2008**, *141*, 577–587. [CrossRef]
17. Rosset, S.; Araromi, O.A.; Schlatter, S.; Shea, H.R. Fabrication process of silicone-based dielectric elastomer actuators. *J. Vis. Exp.* **2016**, *108*. [CrossRef] [PubMed]
18. Bozlar, M.; Punckt, C.; Korkut, S.; Zhu, J.; Chiang Foo, C.; Suo, Z.; Aksay, I.A. Dielectric elastomer actuators with elastomeric electrodes. *Appl. Phys. Lett.* **2012**, *101*, 091907. [CrossRef]
19. He, X.; Gao, W.; Xie, L.; Li, B.; Zhang, Q.; Lei, S.; Robinson, J.M.; Haroz, E.H.; Doorn, S.K.; Wang, W.; et al. Wafer-scale monodomain films of spontaneously aligned single-walled carbon nanotubes. *Nat. Nanotech.* **2016**, *11*, 633. [CrossRef] [PubMed]
20. Cho, D.Y.; Eun, K.; Choa, S.H.; Kim, H.K. Highly flexible and stretchable carbon nanotube network electrodes prepared by simple brush painting for cost-effective flexible organic solar cells. *Carbon* **2014**, *66*, 530–538. [CrossRef]
21. Ramasamy, E.; Lee, W.J.; Lee, D.Y.; Song, J.S. Spray coated multi-wall carbon nanotube counter electrode for tri-iodide (I3-) reduction in dye-sensitized solar cells. *Electrochem. Commun.* **2008**, *10*, 1087–1089. [CrossRef]
22. Nobusa, Y.; Yomogida, Y.; Matsuzaki, S.; Yanagi, K.; Kataura, H.; Takenobu, T. Inkjet printing of single-walled carbon nanotube thin-film transistors patterned by surface modification. *Appl. Phys. Lett.* **2011**, *99*, 183106. [CrossRef]
23. Shigemune, H.; Maeda, S.; Hara, Y.; Hosoya, N.; Hashimoto, S. Origami robot: A self-folding paper robot with an electrothermal actuator created by printing. *IEEE/ASME Trans. Mechatron.* **2016**, *21*, 2746–2754. [CrossRef]
24. Shigemune, H.; Maeda, S.; Cacucciolo, V.; Iwata, Y.; Iwase, E.; Hashimoto, S.; Sugano, S. Printed paper robot driven by electrostatic actuator. *IEEE Robot. Autom. Lett.* **2017**, *2*, 1001–1007. [CrossRef]
25. Ryokai, K.; Marti, S.; Ishii, H. I/O brush: Drawing with everyday objects as ink. In Proceedings of the SIGCHI Conference on Human Factors in Computing Systems, Vienna, Austria, 24–29 April 2004.
26. Enomae, T.; Han, Y.; Isogai, A. Nondestructive determination of fiber orientation distribution of paper surface by image analysis. *Nord. Pulp Pap. Res. J.* **2006**, *21*, 253. [CrossRef]